Progress in Organic Coatings 74 (2012) 405–409

Contents lists available at SciVerse ScienceDirect

Progress in Organic Coatings

journal homepage: www.elsevier.com/locate/porgcoat

Insights into protection mechanisms of organic coatings from thermal testing with EIS

Zalilah Sharer[a,b,*], John Sykes[a]

[a] Department of Materials, University of Oxford, Parks Road, OX1 3PH Oxford, UK
[b] Department of Gas Engineering, University of Technology Malaysia, 81310 Johor, Malaysia

ARTICLE INFO

Article history:
Received 12 May 2011
Received in revised form 6 December 2011
Accepted 7 December 2011
Available online 26 February 2012

Keywords:
EIS
Organic coating
Free film
Thermal testing
Potentiostatic pulse test

ABSTRACT

The proposition that corrosion rate is limited by the ionic resistance of an organic coating has been tested. Mild steel panels coated with an epoxy-phenolic paint were exposed to 3% sodium chloride solution at 50 °C for different periods and characterized by electrochemical impedance spectroscopy (EIS) across a range of temperatures (25–50 °C). Changes in the film resistance and charge-transfer resistance with temperature were analysed to deduce activation energies for the processes involved. It was found that the calculated activation energy from coating resistance is significantly lower than the activation energy for the charge transfer resistance. This suggests that the ionic resistance of the coating, as apparent in an AC measurement, cannot be controlling the corrosion rate. Coating resistances for free films of the same coating show even higher activation energy values, so that the resistance of un-degraded areas of the coating within the current path could be controlling the current flow. Potentiostatic pulse tests on coated metal have enabled iR-corrected polarization curves to be plotted at different temperatures that gave high activation energies from the estimated corrosion currents. This provides two possible explanations that can account for the results.

1. Introduction

The link between the coating resistance (as measured on a steel substrate) and protective ability of paints was first demonstrated by Bacon et al. [1]. This has lead to use of AC methods to assess the performance of coatings systems. Mayne [2] rationalized this correlation in terms of "resistance inhibition" by which the resistance to a flow of ions between anode and cathode controlled the corrosion process. According to this model corrosion current passes through the coating twice; at the anodes and at the cathodes, so that even if the ionic resistance at the anodes (say) is low, a high ionic resistance above the cathodes would limit the corrosion current passing between anode and cathode. Because current passes through both we can see that the anode and cathode impedance add in series in the galvanic circuit.

Here we have used the effect of high temperature tests both to speed up degradation and to generate activation energies that can be used to identify mechanism. High temperature exposure coupled with EIS has been used before as a useful way to accelerate testing [3]. More recently, Bierwagen et al. [4] used EIS and temperature cycling to further speed up coating breakdown. Ochs and Vogelsang [5] used 'relaxation voltammetry' at different temperatures to determine activation energy from coating resistance and concluded that coating resistance can exhibit a very high activation energy that increases for thicker coatings. In this work, we have exposed coated steel panels at 50 °C to accelerate the test but measured impedance spectra for coated steel panels across a range of temperatures to determine the activation energy for ion conduction and the corrosion process. Changes in impedance parameters were monitored as corrosion began and the coating properties became degraded. Further short term investigations were made on free films to determine the activation energy for ion conduction in un-degraded coating.

In the potentiostatic pulse test (PPT), potentials were applied in a series of steps (anodic or cathodic) from the free corrosion potential. Correction of the potential was carried out, to compensate for ohmic potential drop due to the high resistance of the coating, so that corrected polarization curves could be plotted. PPT can be used to measure responses of current under transient state but in this work, it is used only to determine steady currents after a fixed time of polarization to plot polarization curves for reactions beneath the coating. The step method minimizes interference from charging of the coating capacitance.

* Corresponding author at: Department of Materials, University of Oxford, Parks Road, OX1 3PH Oxford, UK. Tel.: +44 01865 273788; fax: +44 01865 273789.
E-mail addresses: zalilah.bintisharer@materials.ox.ac.uk (Z. Sharer), john.sykes@materials.ox.ac.uk (J. Sykes).

0300-9440/$ – see front matter © 2011 Published by Elsevier B.V.
doi:10.1016/j.porgcoat.2011.12.002

2. Experimental details

2.1. Attached film

In this work, a commercial polyamide adduct cured epoxy-phenolic paint with 150 μm thickness was tested. Coatings were applied to grit-blasted mild steel panels by air spraying. The edges were protected with a thick high-performance epoxy coating. The electrochemical measurements were made using a three-electrode cell. The working electrode had a working area of 40 cm^2, the reference electrode was a saturated calomel electrode (SCE) and the counter electrode was a platinized titanium electrode with an area of 9 cm^2. The sample was placed vertically in hot 3 wt% sodium chloride solution (800 cm^3), made from analytical grade NaCl and deionized water, held at constant temperature in a water bath (or slowly cooled in an insulated box).

The impedance measurements were taken with a Gill AC computer-controlled potentiostat with a high-impedance paint buffer system (ACM Instruments). Tests were carried out at the free corrosion potential for temperatures from 50 °C down to ambient with a 20 mV signal amplitude over a frequency range from 0.1 Hz to 30 kHz, with 25 points in logarithmic decrements. After samples had been tested, the cell was replaced in the hot water bath and kept constant at 50 °C until the next measurement.

2.2. Free film

Free films (150 μm thick) were prepared by casting the epoxy-phenolic paint onto a degreased sheet of thick silicone rubber using a draw-down bar. Adhesion to the rubber is poor and coatings could be easily peeled off. For measurements on the free-standing film the sample was clamped between silicone rubber gaskets (exposing 7.06 cm^2) in a two-compartment cell and a two-electrode arrangement was used, with one Ag/AgCl electrode acted as both counter electrode and reference electrode and the other as working electrode. The spectrum was obtained with zero DC offset using frequency range 1 Hz to 30 kHz and AC amplitude of 10 mV. Exposure tests were conducted at 40 °C and EIS measurements were taken across a range of temperature (21–40 °C). Then the same film was exposed at 21 °C and EIS measurements were taken across a lower range of temperatures (10–21 °C).

2.3. Equivalent circuit

The EIS spectra from attached films were analysed using non-linear least squares fitting (with ZSimWin) to a *R*[*Q*[*R*[*QR*]]] model circuit as illustrated in Fig. 1a [*Q* = constant phase element]. This is typical circuit used for coated metals with a conducting pathway (or pore) modelled as a resistance in series with a parallel RC combination at the metal surface to represent the electrochemical reaction there (or more recently RQ to represent non-ideal behaviour). The capacitance (or *Q*) of the organic coating is arranged in parallel with this combination and short-circuits the whole combination at high frequency. EIS spectra from free films which should in principle be fitted *R*[*QR*] as illustrated in Fig. 1b, but were actually analysed with the circuit in Fig. 1a which gave a better fit. The small additional term may originate in the impedance of the test electrodes.

2.4. Potentiostatic pulse test (PPT)

The rest potentials of the epoxy-phenolic attached films were measured at the beginning of the test. Then a series of potential steps (typically 100–600 mV) were applied from the rest potential. The resulting current was measured every second for a period of 300 s to allow the current to stabilize, before applying another potential step. Before each PPT measurement, EIS tests were conducted to determine the coating resistance which is necessary for iR-correction.

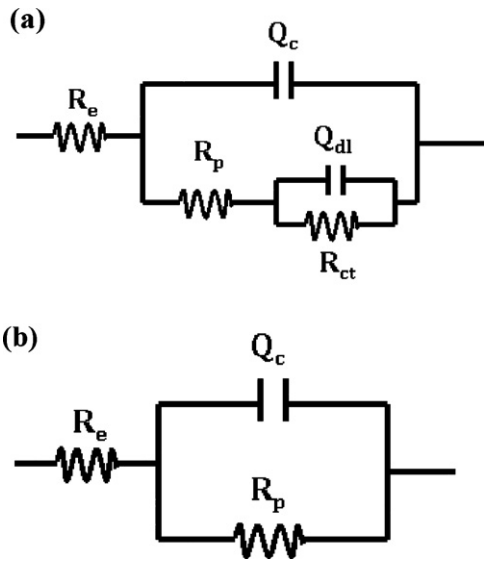

Fig. 1. Model circuit for (a) an attached film and (b) a free film.

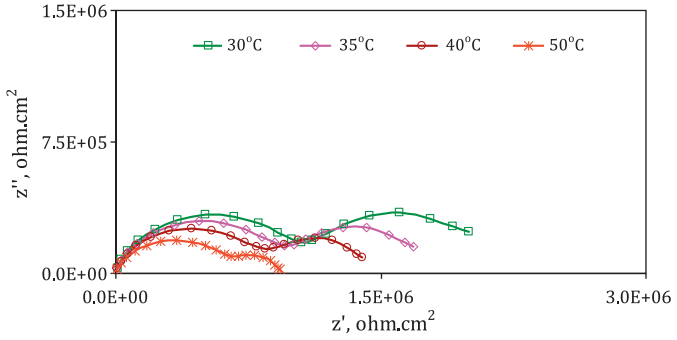

Fig. 2. Nyquist plots at various temperatures for epoxy-phenolic coating after 14 days of exposure at 50 °C.

3. Results

3.1. Attached film

Figs. 2 and 3 show the effect of temperature on EIS response of an epoxy-phenolic coated steel panel after 14 and 30 days exposure at 50 °C. These show two semicircles which both shrink in size as temperature rises. These plots were fitted to the equivalent

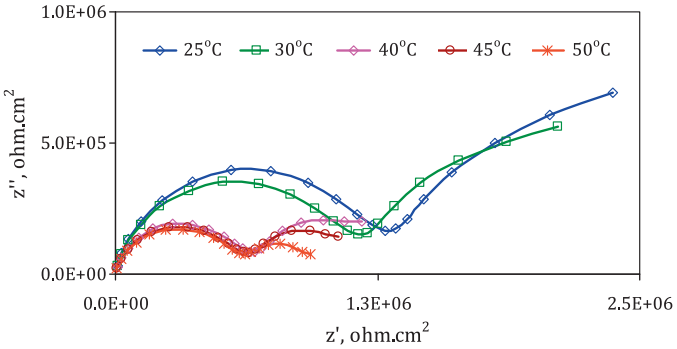

Fig. 3. Nyquist plots at various temperatures for epoxy-phenolic coating after 30 days of exposure at 50 °C.

Table 1
Parameters for epoxy-phenolic coating from fitting of EIS after 14 days at 50 °C.

T (°C)	Q_c (Ss^n cm^{-2})	n	R_p (Ω cm^2)	Q_{dl} (Ss^n cm^{-2})	n	R_{ct} (Ω cm^2)
30	1.27E−09	0.803	9.04E+05	2.82E−07	0.579	2.25E+06
35	1.38E−09	0.801	8.03E+05	2.86E−07	0.579	1.84E+06
40	1.51E−09	0.799	6.94E+05	2.82E−07	0.575	1.48E+06
50	1.83E−09	0.795	4.90E+05	2.20E−07	0.575	9.39E+05

Table 2
Parameters for epoxy-phenolic coating from fitting of EIS after 30 days at 50 °C.

T (°C)	Q_c (Ss^n cm^{-2})	n	R_p (Ω cm^2)	Q_{dl} (Ss^n cm^{-2})	n	R_{ct} (Ω cm^2)
25	1.26E−09	0.803	1.14E+06	5.87E−07	0.546	4.14E+06
30	1.38E−09	0.798	1.02E+06	6.28E−07	0.537	3.43E+06
40	1.69E−09	0.795	5.54E+05	8.01E−07	0.513	1.52E+06
45	1.84E−09	0.791	5.23E+05	7.72E−07	0.512	1.28E+06
50	2.05E−09	0.788	4.88E+05	6.18E−07	0.519	1.00E+06

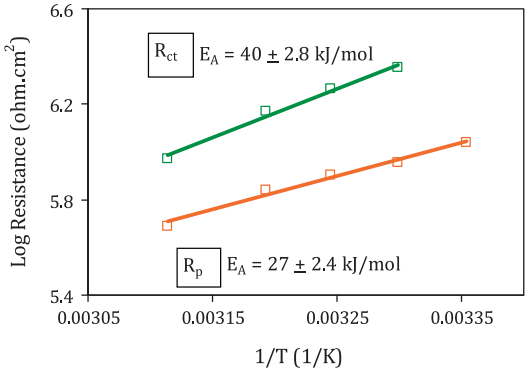

Fig. 4. Arrhenius plot of R_p and R_{ct} for epoxy-phenolic coating after 14 days of exposure.

circuit in Fig. 1a and the resulting parameters are listed in Tables 1 and 2. This procedure gives the most accurate determination of coating resistance (high frequency) and charge transfer resistance (low frequency). Then the logarithm of R_p (coating resistance) and logarithm of R_{ct} (charge transfer resistance) were plotted against reciprocal of temperature to determine activation energies for conduction in the coating and the corrosion reaction. A straight line was fitted to the data points in Figs. 4 and 5 to calculate the activation energy for conduction in the film (from R_p) and for the corrosion process (from R_{ct}); found by multiplying the slope with the gas constant, R.

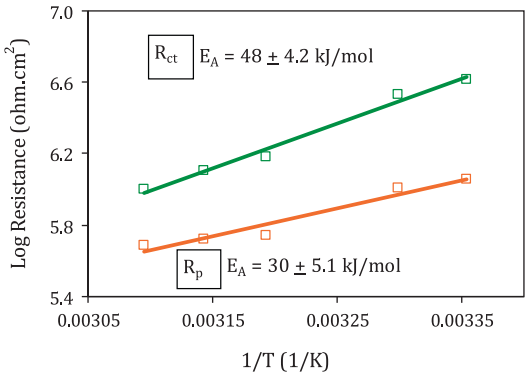

Fig. 5. Arrhenius plot of R_p and R_{ct} for epoxy-phenolic coating after 30 days of exposure.

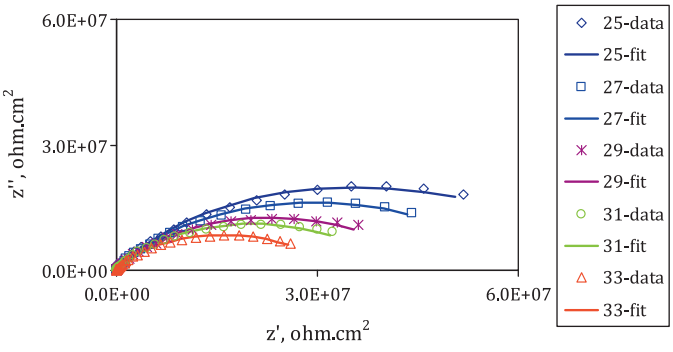

Fig. 6. Nyquist plot at various temperatures for free film exposed at (21–40 °C) with fitted curves.

3.2. Free film

Figs. 6 and 7 show EIS responses for freestanding film at various temperatures, during exposure to 3% NaCl solution. The semi-circle in the Nyquist plots once again becomes smaller at higher temperature. To assess the influence of the temperature on the ion conduction, these semi-circles were first fitted with a model circuit as shown in Fig. 1b, but $R[QR]$ does not fit the data well at lower frequency values, so the other equivalent circuit $R[Q[R[QR]]]$ (Fig. 1a) was used and a good agreement was observed between the experimental data and the fit (Fig. 6). The fitted parameters are summarized in Tables 3 and 4. As two time constants were used and considering that free film normally gives one time constant, the film resistance is taken as the sum of R_f and R_1 together, but in any case the second term is negligibly small. When $\log(R_f)$ was plotted against $1/T$ a good straight line was again observed (Figs. 8 and 9), which indicates a good fit to the Arrhenius equation and enables

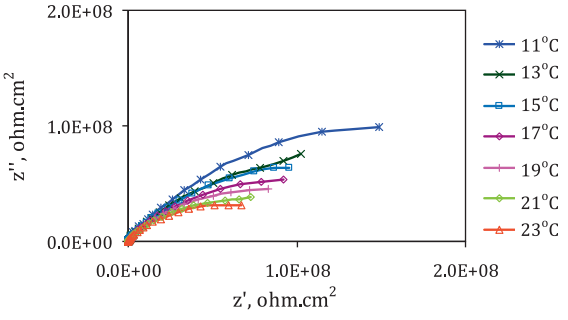

Fig. 7. Nyquist plot at various temperatures for free film exposed at (10–23 °C).

Table 3
Best fit parameters for free film exposed at (40–21 °C) in NaCl solution.

T (°C)	Q_1 (Ss^n cm^{-2})	n	R_1 (Ω cm^2)	Q_f (Ss^n cm^{-2})	n	R_f (Ω cm^2)
25	5.58E−11	1	5.04E+05	2.34E−09	0.609	7.31E+07
27	5.65E−11	1	4.49E+05	2.55E−09	0.605	5.99E+07
29	5.90E−11	1	4.42E+05	2.87E−09	0.605	4.65E+07
31	6.20E−11	1	4.71E+05	3.05E−09	0.601	4.11E+07
33	3.56E−11	1	3.42E+04	3.50E−09	0.597	3.25E+07

Table 4
Best fit parameters for free film exposed at (10–23 °C) in NaCl solution.

T (°C)	Q_1 (Ss^n cm^{-2})	n	R_1 (Ω cm^2)	Q_f (Ss^n cm^{-2})	n	R_f (Ω cm^2)
11	4.65E−11	1	9.16E+05	1.11E−09	0.644	3.57E+08
13	1.02E−10	0.920	1.46E+04	1.62E−09	0.568	3.13E+08
15	3.09E−11	1	3.80E+04	1.43E−09	0.638	2.28E+08
17	4.90E−11	1	6.13E+05	1.64E−09	0.619	1.87E+08
19	5.19E−11	1	7.02E+05	1.72E−09	0.621	1.56E+08
21	3.11E−11	1	2.99E+04	1.79E−09	0.631	1.28E+08
23	3.11E−11	1	3.78E+04	1.99E−09	0.626	1.13E+08

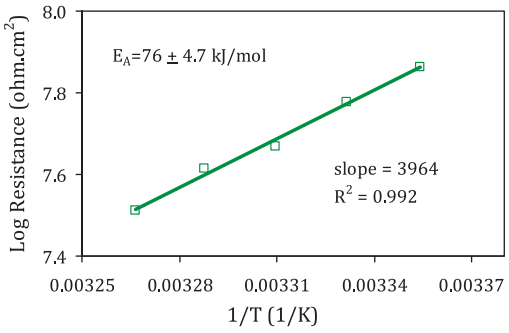

Fig. 8. Arrhenius plot for free film exposed at (40–21 °C) in NaCl solution.

E_A to be calculated. Similar E_A values are obtained, irrespective of whether the film is heated or cooled.

3.3. Potentiostatic pulse measurements

The potentials were corrected by subtracting the iR drop calculated from the product of the steady state current and the coating resistance, as determined from the earlier EIS measurement, then plotted vs. log(current). The effect of temperature on anodic and cathodic polarization after iR correction is presented in Fig. 10. It can be seen that anodic curve is not strongly affected by the temperature change. The influence of temperature is more evident on the cathodic curve (Fig. 10b) where the cathodic current density becomes larger as the temperature rises. The cathodic current density for each temperature was determined from the Tafel line at a fixed potential (E = −650 mV). Logarithm of current density is then

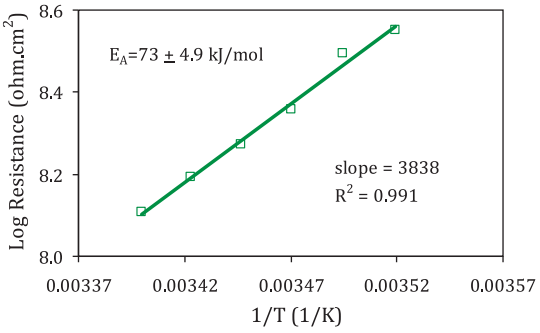

Fig. 9. Arrhenius plot for free film exposed at (10–23 °C) in NaCl solution.

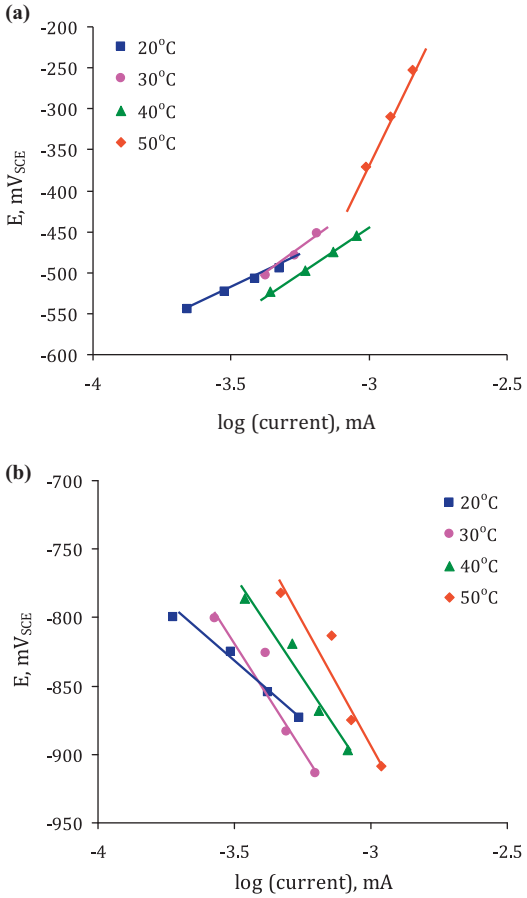

Fig. 10. Effect of temperature changes on (a) anodic and (b) cathodic curves of epoxy-phenolic coating.

plotted against the reciprocal of temperature and a straight line indicates that the current obeys the Arrhenius law (Fig. 11) with $E_A = 66 \pm 2$ kJ mol^{-1}.

4. Discussion and conclusions

As presented in Table 5, the Arrhenius plots of temperature dependence for ion transport (from R_p) exhibited different slopes than those for the corrosion process (from R_{ct}) with the latter significantly higher. This suggests that the coating resistance being measured here cannot be the factor controlling the corrosion rate.

This raises a question then; what is controlling the corrosion rate? One option can still be based on Mayne's resistance inhibition model in which the current flows twice through the paint–at the anode and at the cathode. Even if the coating is initially

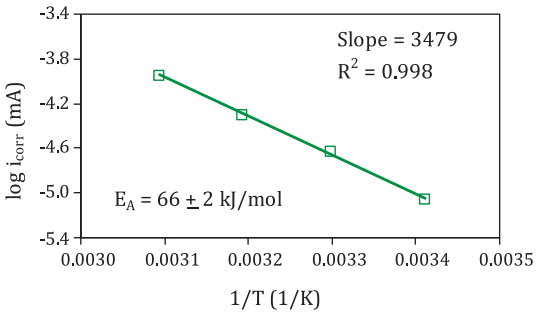

Fig. 11. Arrhenius plot calculated from cathodic Tafel line.

Table 5
Activation energy determined from EIS and PPT test.

Sample	EIS		PPT
	E_A from R_p (kJ mol^{-1})	E_A from R_{ct} (kJ mol^{-1})	E_A from i_{corr} (kJ mol^{-1})
Attached film	27–30	40–48	66
Free film	73–76		

uniform (which would be unusual), we expect corrosion to initiate at pores or other defects in the coating, and the cathode reaction to then take place elsewhere. Because the processes at anode and cathode are quite different they will have different effects on the coating resistance. So, for one reason or another, the likelihood is that coating resistance will be different at the anodes and the cathode. The lower resistance is the only one that can be measured in EIS – it short circuits the other higher resistance – but actually the higher resistance is the one that would control the corrosion rate if resistance inhibition were the controlling mechanism, as expected for a simple barrier coating under immersion conditions. In the EIS measurements R_a (anode) and R_c (cathode) are in parallel, but in the corrosion cell they act in series.

Free film tests show that for un-degraded coating, freshly exposed and not in contact with a metal substrate, a higher activation energy for ion transport is observed (73–76 kJ mol^{-1}). This might indicate that if current has to pass through less degraded areas of coating of higher resistance as it passes from anode to cathode, the corrosion current will depend upon this higher resistance that also shows a high dependence on temperature; so if this resistance controls the corrosion rate a high activation energy will be observed for R_{ct}. E_A values for conduction in 'good' region of the coating would need to be intermediate between the pristine free film and the more degraded areas of coating.

This also means that the lower resistance that is being measured doesn't tell whether the coating is still protective or not.

An alternative possibility is that the kinetics of the cathodic reaction on the electrode could be controlling the corrosion rate, rather than the film resistance. Potentiostatic pulse tests have showed that the anode is not really affected by the temperature but oxygen reduction at the cathode is. The activation energy value generated for the cathode reaction is higher than for ion transport from R_p in paint on steel, but more than for the change in R_{ct}.

Acknowledgements

We are grateful to Ministry of Higher Education of Malaysia and University Technology of Malaysia for awarding the scholarship that supported this research and Shell Global Solutions International BV for providing the samples and financial support.

References

[1] R.C. Bacon, J.J. Smith, F.M. Rugg, Ind. Eng. Chem. 40 (1948) 161.
[2] J.E.O. Mayne, Anti-Corros. Methods Mater. 20 (1973) 3.
[3] G.W. Walter, Corros. Sci. 32 (1991) 1085.
[4] G.P. Bierwagen, L. He, J. Li, L. Ellingson, D.E. Tallman, Prog. Org. Coat. 39 (2000) 67.
[5] H. Ochs, J. Vogelsang, Electrochim. Acta 49 (2004) 2973.